Nanoscale

PAPER

Cite this: *Nanoscale*, 2015, **7**, 4956

The mapping of yeast's G-protein coupled receptor with an atomic force microscope

Musashi Takenaka,[a] Yusuke Miyachi,[b] Jun Ishii,[c] Chiaki Ogino*[a] and Akihiko Kondo[a]

Received 9th October 2014,
Accepted 5th February 2015

DOI: 10.1039/c4nr05940a

www.rsc.org/nanoscale

An atomic force microscope (AFM) can measure the adhesion force between a sample and a cantilever while simultaneously applying a rupture force during the imaging of a sample. An AFM should be useful in targeting specific proteins on a cell surface. The present study proposes the use of an AFM to measure the adhesion force between targeting receptors and their ligands, and to map the targeting receptors. In this study, Ste2p, one of the G protein-coupled receptors (GPCRs), was chosen as the target receptor. The specific force between Ste2p on a yeast cell surface and a cantilever modified with its ligand, α-factor, was measured and found to be approximately 250 pN. In addition, through continuous measuring of the cell surface, a mapping of the receptors on the cell surface could be performed, which indicated the differences in the Ste2p expression levels. Therefore, the proposed AFM system is accurate for cell diagnosis.

Introduction

Biomolecule interactions usually trigger a signal transduction for the alternation of physiological functions.[1,2] To analyze these functions, methods of analysis that focus on interactions such as protein–protein affinities have been developed as follows: Surface Plasmon Resonance (SPR) analysis[3,4] and Quartz Crystal Microbalance (QCM) analysis.[5,6] For both of these types of analysis, an interactive force between molecules can be measured on the chip surface and analyzed quantitatively. Since there are no requirements for the chemical modification of target molecules with fluorescent dyes or radioisotopes, these are usually used for evaluation. Recently, the simultaneous imaging and analysis of interactions between molecules has been required, particularly on the surfaces of cell membranes, which is assumed to be difficult with SPR and QCM. On the other hand, an AFM can be used for the imaging of a sample while also measuring the interaction force on a cell membrane.

The AFM was intended for high-resolution imaging when it was first developed[7] in 1986. Since the imaging of a cell by an AFM was first reported[8] in 1995, the methodology for cell imaging has been further developed.[9–12] For stable cell imaging, Ikai's group attempted to immobilize cells on a glass surface using a syringe.[8] After that, a cell-immobilizing methodology was often performed using agarose[9] or gelatins.[10,11] In addition, the use of a cell-imprinting methodology has also been reported.[12] On the other hand, the elasticity of a cell membrane has been gauged through a combination of cell immobilization and measurement of the interaction.[10] As for a protein expressed on a cell surface, the sensor protein Wsc1 on a yeast cell surface[16] or EGFR[17] has been targeted. In each study, one kind of cell was employed, while, in the proposed study, the mutants with different expression levels of G-Protein Coupled Receptor (GPCR) are employed and compared for the first time. The following procedures were used to evaluate a molecule–molecule interaction through modification of the cantilever with a linker molecule: affinity evaluation of the streptavidin–biotin complex,[13] enzymatic nanolithography of the FRET peptide layer,[14] and direct observation of substrate–enzyme complexation.[15]

GPCRs are well known as target receptors for ligands, and yeast's GPCR, Ste2p, was generally targeted as a model of GPCR. GPCRs are membrane translocate proteins that form 7-transmembrane domains and have a common mechanism for signal transduction.[18–20] When GPCRs interact with a ligand outside of the cell membrane, they activate an inside signal transduction pathway and induce a cellular response. Because of their important role in cellular physiology, GPCRs have been targeted for use with medication.[18] We reported a GPCR assay system that focuses on the yeast GPCR, Ste2p.[19,20] This GPCR is expressed on the cell membrane of a mating type of cell haploid, *Saccharomyces cerevisiae*. The mating pheromone secreted from α-mating types of haploid cells, α-factor, is well known to the ligand of Ste2p. In addition, we also employed BY4741*ste2*Δ and BY4741/pGK421-STE2. BY4741*ste2Δ* was the strain knocked out of the *Ste2p* gene. BY4741/pGK421-STE2 is

[a]*Department of Chemical and Engineering, Graduate School of Engineering, Kobe University, Kobe, Japan. E-mail: ochiaki@port.kobe-u.ac.jp*
[b]*Department of Biotechnology, Graduate School of Engineering, Nagoya University, Nagoya University, Nagoya, Japan*
[c]*Organization of Advanced Science and Technology, Kobe University, Kobe, Japan*

This journal is © The Royal Society of Chemistry 2015

the strain over-expressed Ste2p by introducing the constructed plasmid, pGK421-STE2. Although a lot of knowledge of Ste2p has been reported in the previous papers, the quantitative analysis of Ste2p had not been performed, and one semi-quantitative analysis of recombinant tagged-Ste2p by Western blotting analysis was just reported.[21] Therefore, there have been no reports about the quantitative analysis of native Ste2p.

In the present study, the evaluation of Ste2p density and the differences in the Ste2p expression levels in yeast were performed using an AFM. At first, the fluorescence intensities were measured using α-factor-modified fluorescent dye. Thereafter, *via* the α-factor-modified cantilever, the yeast strains expressing different Ste2p expression levels were surveyed and the interaction affinities between a yeast cell and the cantilever were measured. Then, we elucidated the relationship between the fluorescence intensities and the interaction affinity forces.

Experimental

Yeast strains and chemicals

S. *cerevisiae* BY4741 [*MAT***a** *his3*Δ*1 leu2*Δ*1 met15*Δ*0 ura3*Δ*0*][22] and the mutant strain BY4741*ste2*Δ [*MAT***a** *his3*Δ*1 leu2*Δ*0 met15*Δ*0 ura3*Δ*0 ste2*Δ::kanMX4][23] were constructed according to a method established in our previous paper,[20] and were used in the present study.

The crosslinking agent for ligand modification with the cantilever was 3,3′ dithiobis[sulfosuccinimidylpropionate] (DTSSP) (Thermo Scientific, Massachusetts, USA), and the pheromone molecule for yeast was α-factor (Zymo research, California, USA). For cultivation or transformation, we used a yeast nitrogen base without amino acids, peptone, or carrier DNA (Takara Bio Inc., Shiga, Japan). In this research, the other chemicals used were of analytical grade (Nacalai Tesque, Kyoto, Japan).

Transformation, cultivation, and immobilization of yeast

The yeast transformation was accomplished *via* the lithium acetate method, as follows.[24]

Cultivation and immobilization for each of the three strains, BY4741 WT, BY4741*ste2*Δ, and BY4741/pGK421-STE2, were performed in the same manner as follows: the yeast strains, two strains, BY4741 WT and BY4741*ste2*Δ, were incubated at 30 °C in 5 mL of YPD medium for 20 h with shaking at 150 rpm; BY4741/pGK421-STE2 was incubated at 30 °C in 5 mL of SD medium (containing 20 mg L^{-1} uracil, 30 mg L^{-1} leucine, 20 mg L^{-1} histidine) for 20 h with shaking at 150 rpm. After cultivation, the cell pellets were collected by centrifugation at 3000 rpm at room temperature for 5 min. The cell pellets were then washed with 5 mL of ultrapure water. They were centrifuged and the supernatant was removed again, then the cell pellets were re-suspended in 100 μL of distilled water. The cell concentration was adjusted to give an optical density of 1.0 at 600 nm (OD_{600} = 1.0) by dilution with ultrapure water.

5 μL of a yeast-cultivated suspension (OD_{600} = 1.0) was dropped onto a ∅13 mm glass slide (referred to here as glass slide (X)) (Matsunami Glass Industries, Tokyo, Japan), and allowed to dry. In a block incubator (ASTEC Corporation, Fukuoka, Japan), 33 mg of soft agarose of electrophoresis experiment grade was diluted in 1 mL SD medium (containing 20 mg L^{-1} uracil, 30 mg L^{-1} leucine, 20 mg L^{-1} histidine and 30 mg L^{-1} methionine, filtered; this medium was also utilized for an AFM), and melted at 100 °C for approximately 30 min. After the agarose had melted, the solution temperature was maintained at 60 °C. After about 30 min of incubation, 20 μL of the agarose solution was dropped onto the glass slide (X) with the immobilized yeast cells. Then, using another glass slide (Y), the agarose solution and the immobilized yeast cells were sandwiched immediately, and it was allowed to stand for 1 min. Then it was turned and the top glass slide (X) was removed (Fig. 1A).

AFM tip modification with α-factor

The cantilever used in the present study was OMCL-TR400PB-1 (Olympus Corporation, Tokyo, Japan). It was 100 μm in length, with a 0.09 N m^{-1} spring constant, a 32 kHz resonant frequency, and gold coating. To clear the organic compounds that may have previously adhered to the cantilever surface, it was treated with ultraviolet (UV) light irradiation for 2 h. The cantilever was then exposed to 100 μL of 4 mg mL^{-1} DTSSP solution in 20 mM acetate (pH 4.8) at room temperature for 30 min. After the reaction, it was dipped in 20 mL ultrapure water to wash out the unreacted DTSSP. The DTSSP-immobilized cantilever was then doused at room temperature with 100 μL of 200 μM α-factor in 20 mM acetate (pH 4.8) for 1 h. After reacting the α-factor with DTSSP, it was dipped in 20 mL of 1 M Tris-HCl (pH 8.0) for 15 min in order to block the unreacted succinimide groups. As a negative control, the succinimide-immobilized cantilever was dipped in 20 mL of 1 M Tris-HCl (pH 8.0) for 75 min. The modified cantilevers were washed with 1 mL SD medium (containing 20 mg L^{-1} uracil, 30 mg L^{-1} leucine, 20 mg L^{-1} histidine and 30 mg L^{-1} methionine, filtered) and were kept in SD medium on ice.

AFM measurement

The glass slide with the immobilized yeast was fastened with double-sided tape on a quart shale, then 1.5 mL of SD medium was poured into it. An SPA400-Nanonavi AFM unit (Hitachi High-Tech Science, Tokyo, Japan) was used, and the dwell time was 10 ms in all measurements. The first approach was operated whereby the cantilever was immediately adjusted to a distance of 200 μm from the target sample. With the optical AFM microscope, the location of the cantilever tip was moved to a point over the yeast cell. Then, topology scanning was performed at a range of 20 μm square with 512 points per line × 512 lines. As a result, the topography of the yeast was obtained. Using an AFM, the location of the cantilever tip could be adjusted to the center of a certain yeast cell, and topography scanning could be repeated for different conditions (6 μm square). When the topography of one yeast cell was obtained, force curve measuring was immediately performed on a 1 μm square of the yeast cell surface with 64 points per line × 64 lines (Fig. 1B). This mode was used to measure the

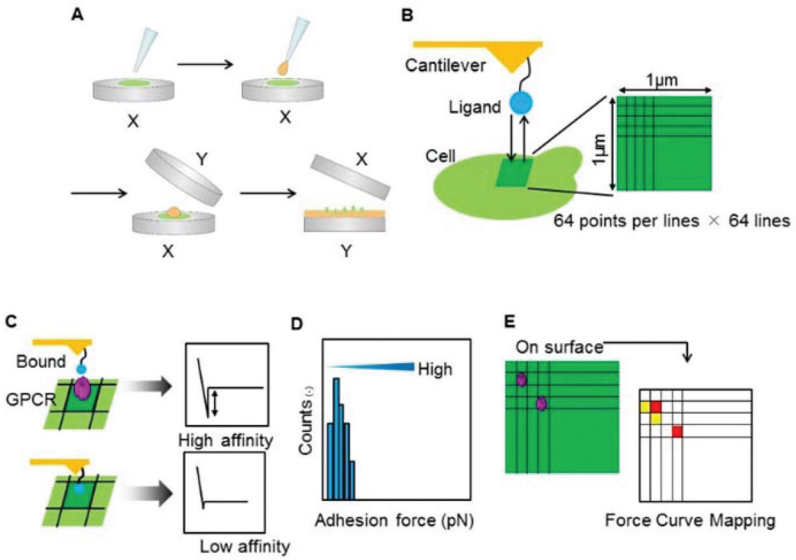

Fig. 1 The measurement scheme in this study. (A) An immobilization of yeast cells on a glass slide. (B) A cantilever modified with a ligand approach to cell surface and force measurement of 4096 points within 1 × 1 μm. (C) The differences in high affinity and low affinity. (D) Histogram. (E) Force curve mapping.

affinity force between the tip of the cantilever and the surface of the yeast cell. A total of 4096 data points were collected on the force curves (Fig. 1C). By using these data sets (affinity force, position information of *X*- and *Y*-axis), a histogram of the adhesion forces could be constructed (Fig. 1D). In addition, the force-curve mapping image was also visualized using a FlexPro7 (Hulinks, Tokyo, Japan) (Fig. 1E).

Cy2-dye labelling of α-factor

To confirm the expression level of the Ste2p receptor in these strains, a fluorescent dye, Cy2-dye (Cy2) (Amersham FluoroLink™ Cy2 Reactive Dye (GE Healthcare, Wisconsin, USA)), was used for the conjugation with α-factor. A sodium carbonate–bicarbonate buffer was prepared according to a procedure established in a previous paper.[25] Then, 1882 μL of this buffer was mixed with 118 μL of 10 mM α-factor. After stirring, 100 μL of this solution was added to a dye vial, and gently mixed at room temperature for 60 min. Then, 2.12 μL of 1 M Tris-HCl (pH 8.0) was additionally mixed for the blocking of unreacted succinimide. After reaction termination, this mixture was stored at 4 °C.

Flow cytometric analysis

The yeasts were harvested and adjusted in the same manner as the cultivation of yeast, as described previously. Then, 100 μL of the Cy2-dye labeling α-factor mentioned above was mixed with these yeast suspensions, and incubated for 3 h at room temperature. On the other hand, as a negative control, the yeasts were prepared in the same manner and then they were mixed with 100 μL of 600 μM α-factor for 3 h.

After reaction, the supernatant was removed completely by centrifugation at 14 000 rpm at room temperature for 5 s, and the precipitant (yeasts) was washed 5 times with 100 μL of phosphate buffer saline (PBS buffer (100 mM phosphate, 600 mM NaCl)). Then, the fluorescence intensities were analyzed using a flow cytometer (BD FACSCantoII; BD Biosciences, CA, USA), as described previously.[20]

Results

Fluorescence intensity of Cy2-dye labelling α-factor

The expression levels of Ste2p were measured as an index of the fluorescence intensity of the Cy2-dye labeled α-factor adsorbed Ste2p on a cell surface. Using flow cytometer analysis, the average fluorescence intensities for 10 000 yeast cells could be measured and quantified (Fig. 2).

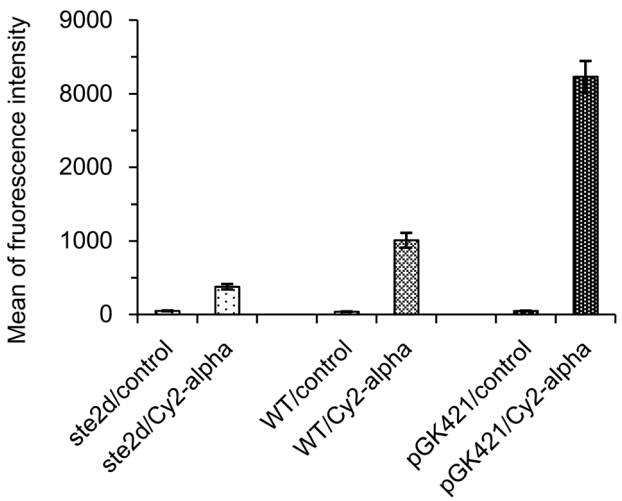

Fig. 2 Comparison of Cy2 fluorescence intensity. The mean Cy2-dye fluorescence of 10 000 cells was measured by flow cytometry. Error bars represent the standard deviation from three separate runs (n = 3).

This journal is © The Royal Society of Chemistry 2015

Each of the average fluorescence intensities depended on the type of transformant. The fluorescence intensities clearly increased as the Ste2p expression level increased. In the case of BY4741*ste2Δ*, there were thought to be no differences between cells either with or without the Cy2-dye labeled α-factor because BY4741*ste2Δ* does not express Ste2p. However, the mean for fluorescence intensity was about 480 with the Cy2-dye labeled α-factor. It was assumed that this was caused by the nonspecific adsorption of the Cy2-dye labeled α-factor. On the other hand, the fluorescence intensity was about 1010 for the complex between BY4741 WT and Cy2-dye labeled α-factor, and the intensity was about 8350 for the complex between BY4741/ pGK421-STE2 and the Cy2-dye labeled α-factor. These intensities were sufficiently large and significantly different. As a result, the fluorescence intensity could indicate the proportion of the expression levels, and the ratio of BY4741 WT to BY4741/pGK421-STE2 was about 1 : 8.

Topographical imaging of yeast cell surface and force curve mapping to indicate Ste2p expression

The yeast BY4741 WT was observed using an AFM equipped with an α-factor-modified cantilever. The topography of the BY4741 WT is shown in Fig. 3A. The topography of the area that is indicated by the black box (in Fig. 3A) is the force

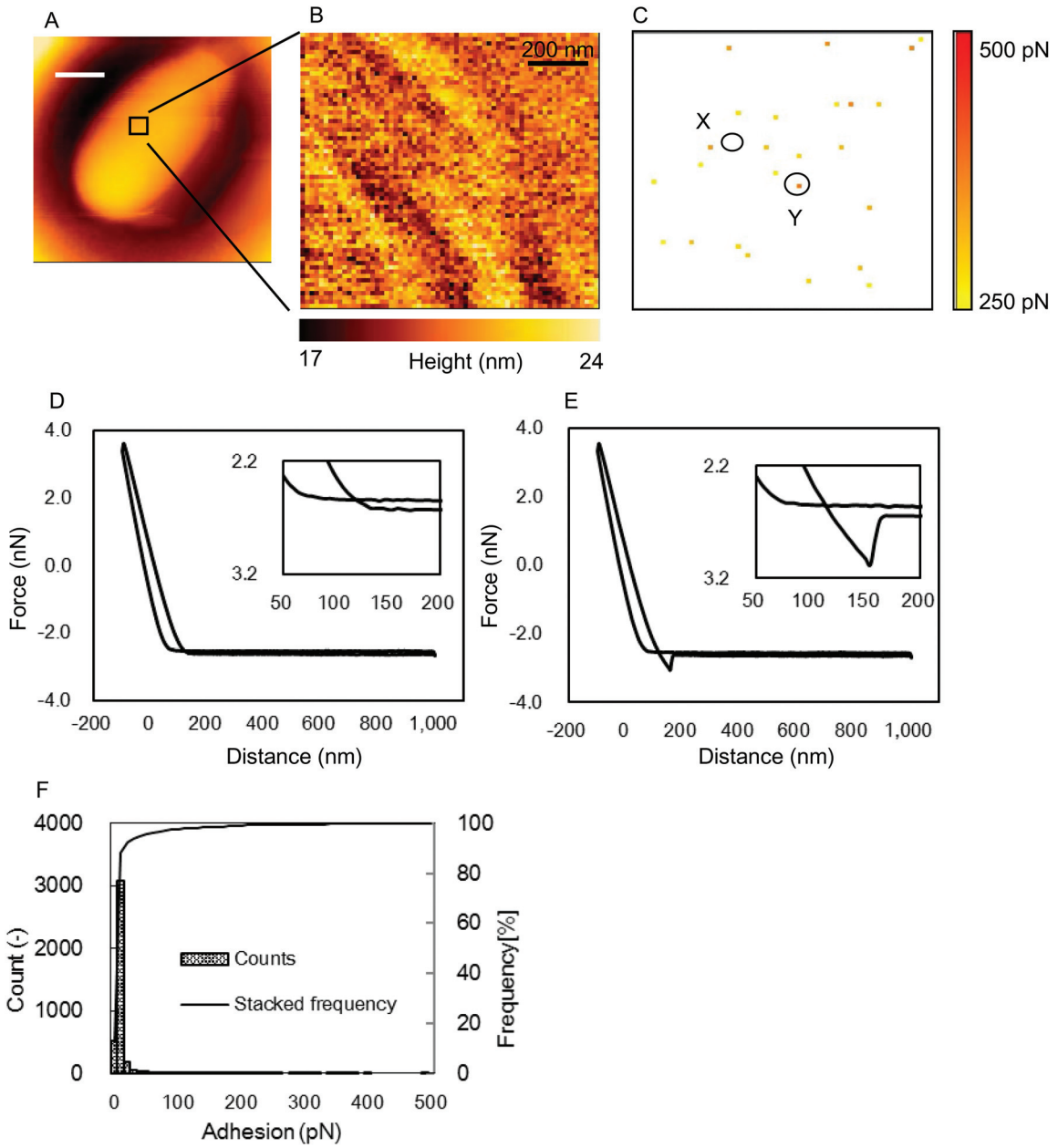

Fig. 3 The methodology for analysis of a force curve with force curve mapping and histograms. (A) The topography of BY4741 WT in 8 μm × 8 μm; (B) the topography of the box in (A); (C) the force curve mapping; (D) one of the force curves not binding (X in (A)); (E) one of the force curves binding (Y in (B)); and, (F) histogram and stacked frequency. The stacked frequency was calculated by (counts)/4096.

curves measuring area (Fig. 3B), and the force curve analysis was carried out for 4096 points within 1 × 1 μm. The analysis was summarized as the force-curve mapping image, as shown in Fig. 3C. The force curves of points X and Y (in Fig. 3C) are shown in Fig. 3D and E, respectively. The roughness of the yeast cell surface was confirmed in Fig. 3B. However, in the same area of the force curve mapping (Fig. 3C), points indicating affinity were confirmed independent of the roughness. Thus, the binding affinity between the α-factor on the tip of the cantilever and Ste2p on the cell surface could be measured using the proposed AFM evaluation system. Point X in Fig. 3C showed a weak force (<200 pN), since no significant affinity force was observed, as in Fig. 3D. However, in the case of Fig. 3E, a strong affinity force was clearly observed (inset in Fig. 3E) at 398 pN for point Y. For the 4096 points of affinity force data, a histogram of the quantitative analysis was also carried out (Fig. 3E). As a result, the Ste2p expression in the targeted area was indicated by the force-curve mapping.

Differences in Ste2p expression levels and Ste2p density

The histograms influence the differences in the Ste2p expression levels (Fig. 4). The stacked frequency was calculated by ∑(counts below the adhesion)/(4096; all counts). The clear differences of the stacked frequency were not confirmed by survey with the no-modified cantilever (Fig. 4B, D, F). On the other hand, the differences were confirmed in the case of

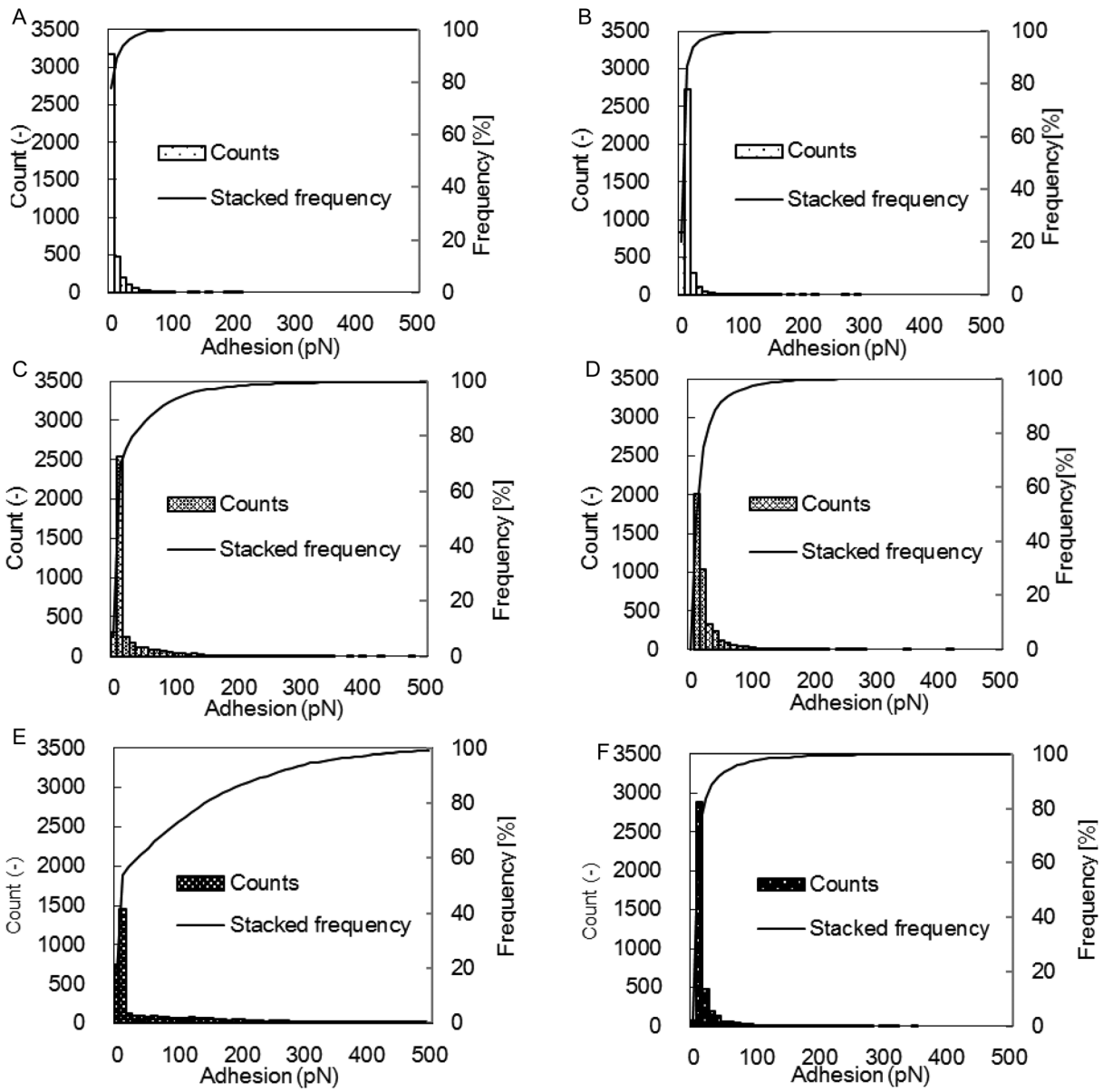

Fig. 4 Histograms. (A) BY4741 ste2Δ with the α-factor-modified cantilever. (B) BY4741 ste2Δ with the no-modified cantilever. (C) BY4741 WT with the α-factor modified cantilever. (D) BY4741 WT with the no-modified cantilever. (E) BY4741/ pGK421-STE2 with the α-factor-modified cantilever. (F) BY4741/pGK421-STE2 with the no-modified cantilever.

This journal is © The Royal Society of Chemistry 2015

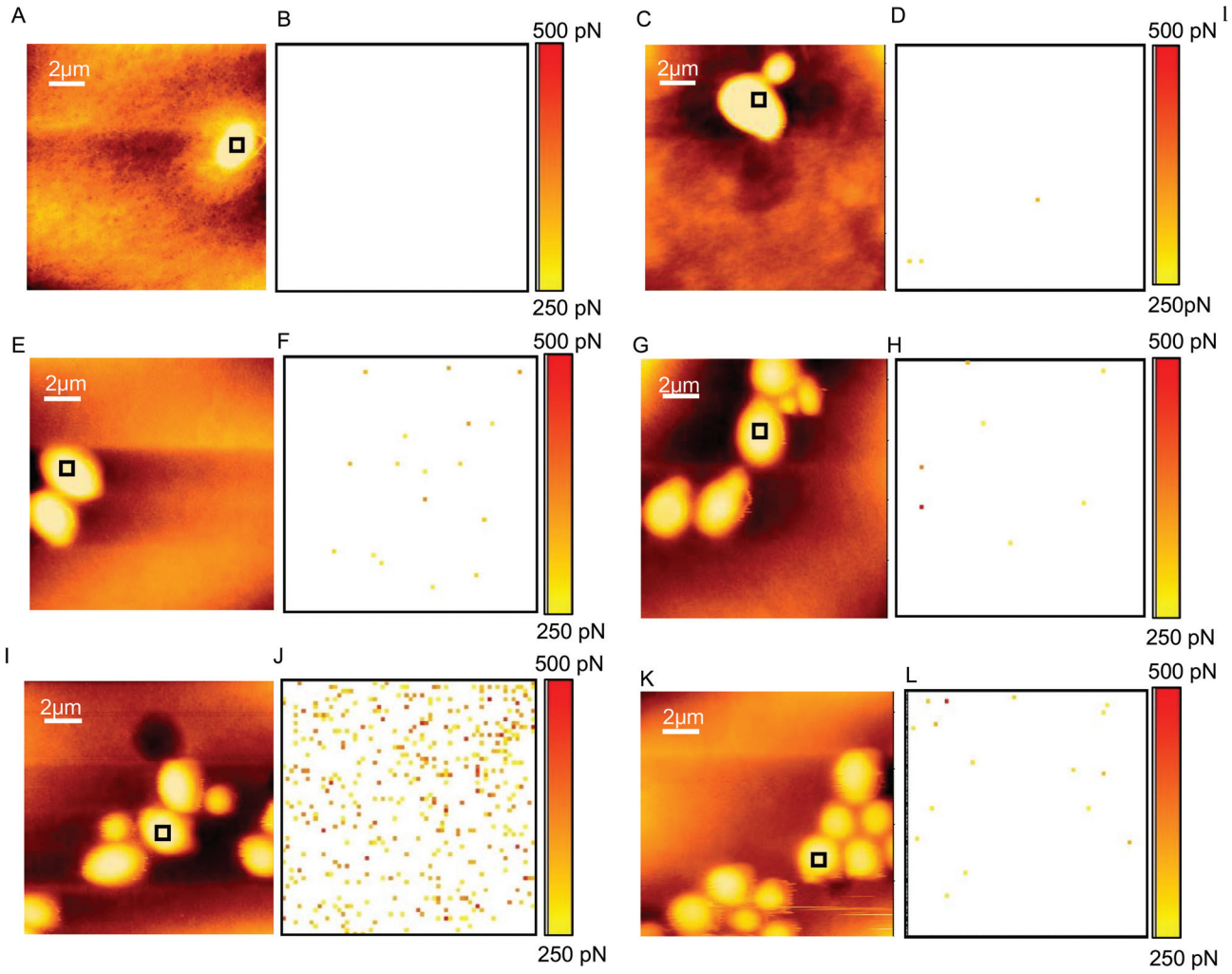

Fig. 5 Force curve mappings. (A) Topography of BY4741 *ste2Δ* with the α-factor-modified cantilever. (B) Force curve mapping in the box area of (A). (C) Topography of BY4741 *ste2Δ* with the no-modified cantilever. (D) Force curve mapping in the box area of (C). (E) Topography of BY4741 WT with the α-factor-modified cantilever. (F) Force curve mapping in the box is from (E). (G) Topography of BY4741 WT with the no-modified cantilever. (H) Force curve mapping in the box area of (G). (I) Topography of BY4741/pGK421-STE2 with the α-factor-modified cantilever. (J) Force curve mapping in the box area of (I). (K) Topography of BY4741/pGK421-STE2 with the no-modified cantilever. (L) Force curve mapping in the box area of (K).

modified α-factor (Fig. 4A, C, E). These differences indicated that it was possible use an AFM to detect the difference in the Ste2p expression levels on the narrow area of a yeast cell surface.

Based on these results, the force curve mapping was indicated (Fig. 5). The colored points indicate the measure of adhesion, and on this point Ste2p and α-factor are supposed to bind so there is Ste2p. No differences were confirmed for either α-factor not modified with a cantilever (Fig. 5D, H, L) or for the knockout strain BY4741*ste2Δ* with the cantilever-modified α-factor (Fig. 5B). On the other hand, many points were confirmed in the case of the over-expressed strain, BY4741/pGK421-STE2 with the cantilever modified α-factor (Fig. 5J). The biased distribution of Ste2p was not confirmed, so Ste2p is expected to express equally. Indeed, the expression level of Ste2p was determined using two methods showing that it targeted the whole yeast cell surface and the narrow yeast cell surface, respectively, and their correlation is shown. We have indicated how to analyze the detected adhesions and the Ste2p expression level in the narrow area using force curve mapping.

Discussion

The adhesion forces between the receptor protein on a cell surface and the cantilever modified with its ligand were first reported and could be applied to the mapping of the receptors. Some adhesion forces between the proteins on a cell surface and proteins modified with a cantilever have been reported.[16,26] In each of these reports, the adhesion forces were found to be on the order of a few hundreds of pN. For example, R. Afrin *et al.* reported that the adhesion force was

about 500 pN between amino-bearing molecules on a cell surface and the cantilever modified with a bifunctional covalent crosslinker.[26] On the other hand, V. Dupres *et al.* reported that it was 162 pN between the sensor proteins on a yeast cell surface and the cantilever modified with Ni^{2+}-NTA groups.[16] In the proposed study, the adhesion force was considered to be between 200 pN and 500 pN between the Ste2p on a yeast cell surface and a cantilever modified with α-factor. The adhesion forces depend on the loading rate, for example, 240 pN s^{-1} in the report of R. Afrin *et al.*[26] and 6.5 pN s^{-1} in the report of V. Dupres *et al.*[16] On the other hand, the loading rate in the present study was 180 nN s^{-1} (multiplying the pulling speed of 2000 nm s^{-1} by the spring constant of 0.09 N m^{-1}). Although the targeted proteins were different, the order of measured adhesion force is considered to be appropriate regarding the loading rate.

The wide range of the adhesion force observed in the case of high interaction force was thought to be caused by the multi-interaction complexes of Ste2p/α-factor. In 4096 force–distance curves of the over-expression strain, several typical force curves were observed (Fig. 6b). We usually observed the 250 pN force with single peak as shown in Fig. 6b-(ii). Therefore, it was assumed to be a single molecule–molecule interaction. In addition, the multi-interaction was also observed as shown in Fig. 6b-(iii, iv, and v). Among them, different force rupture phenomena with same force (around 350 pN) were also observed (Fig. 6b-(iii, and iv)). These results are considered to indicate multi-interactions of receptor–ligand break simultaneously (Fig. 6c-(1)), and the complexes break at different times (Fig. 6c-(2)). Furthermore, the force curve with more than 500 pN was also observed. However, the adhesion force with over 500 pN was never observed, and these results strongly suggested that more than three pairs of complexes would not occur in this experiment.

We first employed the mutants and compared them to statistically analyze the histogram. As for the mutants, the pGK421 plasmid was used and the targeted receptor protein was expressed *via* a multicopy by this plasmid.[19] On the other hand, the fluorescence intensities (Fig. 2) and the counts in the histogram (Fig. 4) were considered to depend on the number of α-factor binding Ste2p. For quantitative comparison, the noise within each of the histogram was eliminated by the adhesion threshold. In each of the histogram with an α-factor-modified cantilever (Fig. 4A, 4C and 4E), the counts above each of the threshold varying from 50 pN to 350 pN were summarized, respectively (Fig. 6a). The percentage of complex formation with over 250 pN in 4096 points with BY4741ste2Δ, BY4741 WT, and BY4741/pGK421-STE2 was calculated as 0.0%, 0.90%, and 9.1%, respectively. The totals of the counts were inversely proportional to the thresholds. In addition, the totals of the counts for BY4741*ste2*Δ became 0 at 250 pN of the threshold. Regarding this point, the count ratio of BY4741 WT to BY4741/pGK421-STE2 at 250 pN of threshold was 1 : 7.5. This ratio is approximately equal to the ratio of the fluorescence intensities (Fig. 4). We could quantitatively evaluate the relationship between the counts and the fluorescence

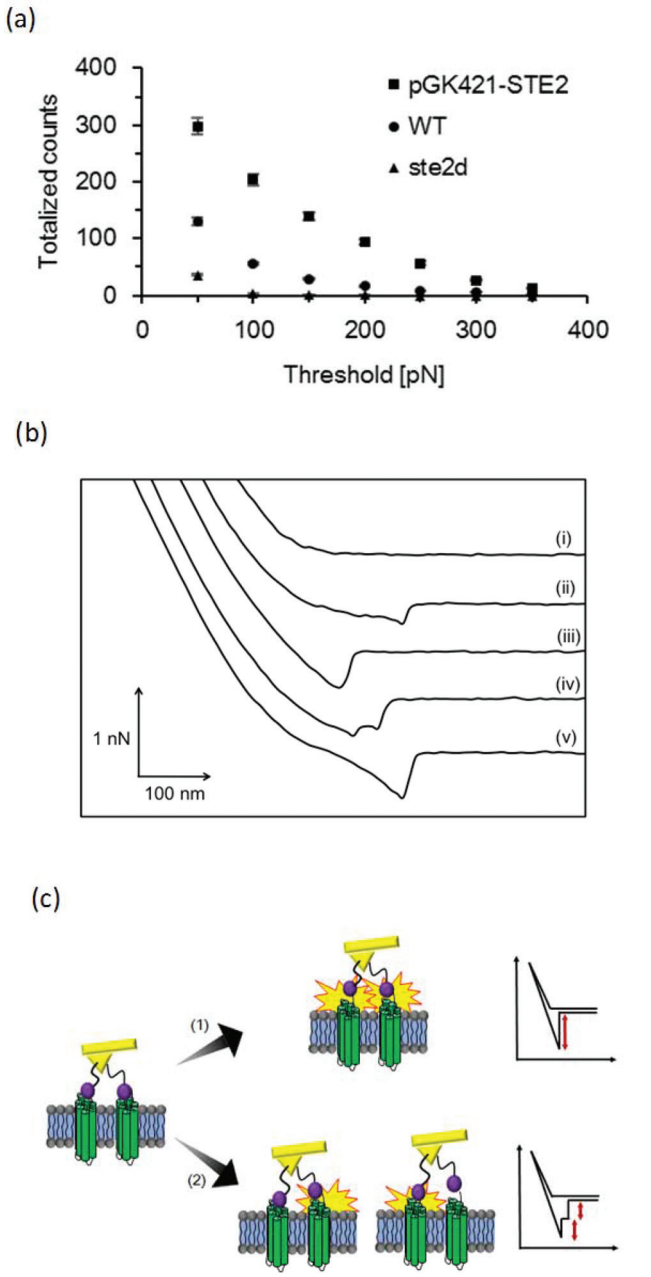

Fig. 6 (a) Comparison the thresholds. The relation between the threshold and the stacked counts. The stacked counts were calculated by summing counts from each threshold to 600 pN. Error bars represent the standard deviation from three separate runs (n = 3). (b) The characteristic force curves of BY4741/pGK421-STE2 with the α-factor modified cantilever (i) 0 pN, (ii) 250 pN, (iii) 1 peak and (iv) 2 peaks with 350 pN, (v) 500 pN. (c) The proposed model force curve: (1) the model of (b-(iii)), and (2) the model of (b-(iv)), respectively.

intensity, which put the specific adhesion forces at above 250 pN between the Ste2p on a yeast cell surface and a cantilever modified with α-factor.

Based on these results, the differences in Ste2p expression were first indicated by force curve mappings. The threshold of 250 pN is considered to be appropriate because the colored

 This journal is © The Royal Society of Chemistry 2015

points indicating the exceeding of this threshold were scarcely seen in the mappings with a no-modified cantilever. On the other hand, the Ste2p expression level depended on the strains, as expected, and then Ste2p was considered to be uniformly expressed. However, the Ste2p expression level of BY4741 WT was less than expected. The Ste2p receptor was well known as the key receptor for the shmoo, which is a singular morphological change.[27] The present study targeted this change, but in the analysis of this change with a single molecule order, the shmoo was infrequent. So the Ste2p expression level of BY4741 was considered inadequate to lead to morphological change, and this mapping indicated Ste2p expression.

As a result, we were able to use an AFM and mapping to accurately indicate the expression of the receptor protein on the yeast cell surface.

Conclusions

The mapping of Ste2p was conducted using an AFM, and the differences in the expression levels on a cell could be indicated. GPCRs are targeted by half of all medicines, and by using genetically engineering methods, some GPCRs can be expressed on a yeast surface. Therefore, this methodology can be applied to the screening of medicines. If the methods that are used to immobilize mammalian cells on glass slides can be refined, this methodology in conjunction with the use of an AFM could become a strong tool for detecting cell surface receptors in the near future.

Acknowledgements

This study was supported in part by a Grant-in-Aid from the Ministry of Education, Culture, Sports, Science and Technology, Japan (no. 19021017 to C.O.), the New Energy and Industrial Technology Development Organization (NEDO) of Japan (no. 06B44019 to C.O.), and by Special Coordination Funds for Promoting Science and Technology, Creation of Innovation Centers for Advanced Interdisciplinary Research Areas (Innovative Bioproduction Kobe), MEXT, Japan.

References

1 M. W. Beukers and A. P. Ijzerman, *Trends Pharmacol. Sci.*, 2005, **26**, 533–539.
2 A. Kiyatkin, E. Aksamitiene, N. I. Markevich, N. M. Borisov, J. B. Hoek and B. N. Kholodenko, *J. Biol. Chem.*, 2006, **281**, 19925–19928.
3 Z. Salamon, H. A. Macleod and G. Tollin, *Biochim. Biophys. Acta*, 1997, **1331**, 117–129.
4 Y. Yanase, H. Suzuki, T. Tsutsui, T. Hiragun, Y. Kameyoshi and M. hide, *Biosens. Bioelectron.*, 2006, **22**, 1081–1086.
5 A. M. Kenneth, *Biomacromolecules*, 2003, **4**, 1099–1120.
6 Z. Pei, J. S. Guitons, C. Kack, B. Ingemarsson and T. Aastrup, *Biosens. Bioelectron.*, 2012, **35**, 200–205.
7 G. Binnig, C. F. Quate and C. Gerber, *Phys. Rev. Lett.*, 1986, **56**, 930–933.
8 S. Kasas and A. Ikai, *Biophys. J.*, 1995, **68**, 1678–1680.
9 T. De, A. M. Chettoor, P. Agarwal, M. V. Salapaka and S. Nettikadan, *Ultramicroscopy*, 2011, **110**, 254–258.
10 P. Schaer-Zammaretti and J. Ubbink, *Ultramicroscopy*, 2003, **97**, 199–208.
11 M. J. Doktycz, C. J. Sullivan, P. R. Hoyt, D. A. Pelletier, S. Wu and D. P. Allison, *Ultramicroscopy*, 2003, **97**, 209–216.
12 X. T. Zhou, F. Zhang, J. Hu, X. Li, X. M. Ma and Y. Chen, *Nanoscale*, 2010, **87**, 1439–1443.
13 C. Yuan, A. Chen, P. Kolb and V. T. Moy, *Biochemistry*, 2010, **39**(33), 10219–10223.
14 C. Nakamura, C. Miyamoto, I. Obataya, S. Takeda, M. Yabuta and J. Miyake, *Biosens. Bioelectron.*, 2007, **22**, 2308–2314.
15 T. Suzuki, Y. W. Zhang, T. Koyama, D. Y. Sasaki and K. Kurihara, *J. Am. Chem. Soc.*, 2006, **128**(47), 15209–15214.
16 V. Dupres, D. Alsteens, S. Wilk, B. Hanse, J. J. heinisch and Y. F. Dufrene, *Nat. Chem. Biol.*, 2009, **5811**, 857–862.
17 S. Lee, J. Mandic and K. J. V. Vliet, *Proc. Natl. Acad. Sci. U. S. A.*, 2007, **104**(23), 9609–9614.
18 A. Wise, K. Gearing and S. Rees, *Drug Discovery Today*, 2002, **7**, 235–246.
19 J. Ishii, S. Matsumura, S. Kimura, K. Tatematsu, S. Kuroda, H. Fukuda and A. Kondo, *Biotechnol. Prog.*, 2006, **22**, 954–960.
20 J. Ishii, M. Moriguchi, K. Y. Hara, S. Shibasaki, H. Fukuda and A. Kondo, *Anal. Biochem.*, 2012, **426**(2), 129–133.
21 B. K. Lee, K. S. Jung, C. Son, H. Kin, N. C. VerBerkmoes, B. Arshava, F. Naider and J. M. Becker, *Protein Expression Purif.*, 2007, **56**, 62–71.
22 C. B. Brachmann, A. Davies, G. J. Cost, E. Caputo, J. Li, P. Hieter and J. D. Boeke, *Yeast*, 1998, **14**, 115–132.
23 A. W. Elizabeth, *et al.*, *Science*, 1999, **285**(5429), 901–906.
24 D. Gietz, A. S. Jean, R. A. Woods and R. H. Schiestl, *Nucleic Acids Res.*, 1992, **20**, 1425.
25 P. L. Southwick, L. A. Ernst, E. W. Tauriello, S. R. Parker, R. B. Mujumdar, S. R. Mujumdar, H. A. Clever and A. S. Waggoner, *Cytometry, Part A*, 1990, **11**, 418–430.
26 R. Afrin, T. Yamada and A. Ikai, *Ultramicroscopy*, 2004, **100**, 187–195.
27 H. Fujimura and N. yanagisawa, *Arch. Microbiol.*, 1983, **136**(1), 79–80.